Computational relativistic quantum dynamics and its application to relativistic tunneling and Kapitza-Dirac scattering

Heiko Bauke,[1, *] Michael Klaiber,[1] Enderalp Yakaboylu,[1] Karen Z. Hatsagortsyan,[1]
Sven Ahrens,[1] Carsten Müller,[1, 2] and Christoph H. Keitel[1]

[1]Max-Planck-Institut für Kernphysik, Saupfercheckweg 1, 69117 Heidelberg, Germany
[2]Institut für Theoretische Physik I, Heinrich-Heine-Universität Düsseldorf, Universitätsstraße 1, 40225 Düsseldorf, Germany

Computational methods are indispensable to study the quantum dynamics of relativistic light-matter interactions in parameter regimes where analytical methods become inapplicable. We present numerical methods for solving the time-dependent Dirac equation and the time-dependent Klein-Gordon equation and their implementation on high performance graphics cards. These methods allow us to study tunneling from hydrogen-like highly charged ions in strong laser fields and Kapitza-Dirac scattering in the relativistic regime.

1. Introduction

With present-day strong lasers [1] providing intensities of the order of 10^{22} W/cm^2 and employing highly charged ions, the regime of relativistic quantum dynamics of strong field processes becomes accessible [2]. The time-dependent Klein-Gordon equation and the time-dependent Dirac equation form the basis for a theoretical description of the relativistic quantum dynamics of spin-zero and spin-half particles, respectively. Deducing analytical solutions of these equations, however, poses a major problem. Analytical methods for determining solutions of these equations usually require physical setups with a high degree of symmetry [3–8]. For the interaction with high-frequency few-cycle laser pulses of high intensity also approximation methods reach their limits. Thus, ultra short laser-matter interactions at relativistic intensities require numerical approaches via computer simulations.

For this purpose, mature methods from nonrelativistic computational quantum dynamics may be transferred into the relativistic regime. However, also new and better methods are needed because relativistic computational quantum dynamics is much more demanding than its nonrelativistic sibling. In this contribution, we survey the challenges of numerical time-dependent relativistic quantum dynamics and present approaches to master these challenges by smart numerical algorithms [9, 10], by high-performance implementations on parallel architectures, including cluster computers and graphics processing cards [9, 11, 12]. Another approach is to cast a quantum system's mathematical description by physical insights into a form that is beneficial for numerical methods [13]. The new methods of computational relativistic quantum dynamics are likely to be beneficial for the emerging field of computational quantum electrodynamics [14].

This contribution is organized as follows. In section 2 we will present numerical approaches to solve time-dependent relativistic quantum equations of motion. Later, some applications of numerical relativistic time-dependent quantum dynamics will be highlighted. The tunneling dynamics in relativistic strong-field ionization will be investigated in section 3 by means of numerical (and analytical) methods to develop an intuitive picture for the relativistic tunneling regime [15]. It is demonstrated that the well-known tunneling picture applies also in the relativistic regime by introducing position dependent energy levels. The time for the formation of momentum components of the ionized electron wave packet (Keldysh time) and the time interval which the electron wave packet spends inside the barrier (Eisenbud-Wigner-Smith time delay) are identified as the two characteristic time scales of relativistic tunnel ionization. The Keldysh time can be related to a momentum shift that is shown to be present in the ionization spectrum at the detector and, therefore, observable experimentally. In section 4 we apply computational relativistic quantum dynamics to study Kapitza-Dirac scattering of electrons by light [16]. In particular, we demonstrate that inelastic scattering processes involving a small odd number of photons are intrinsically relativistic and involve periodic oscillations of the electron's spin degree of freedom.

2. Computational relativistic quantum dynamics

Relativistic quantum dynamics in regimes where the single particle picture is applicable is governed by the Klein-Gordon equation and the Dirac equation. The Klein-Gordon equation, a relativistic generalization of the Schrödinger equation, is an equation

* heiko.bauke@mpi-hd.mpg.de

of motion for a wave function $\Psi(\boldsymbol{r}, t)$ [9, 17]. It governs the evolution of a charged spinless particle with mass m and charge q moving under the effect of electrodynamic potentials $\boldsymbol{A}(\boldsymbol{r}, t)$ and $\phi(\boldsymbol{r}, t)$. Introducing the speed of light c, the Klein-Gordon equation reads in its two-component representation

$$\mathrm{i}\hbar\frac{\partial\Psi(\boldsymbol{r}, t)}{\partial t} = \hat{H}_{\mathrm{KG}}(t)\Psi(\boldsymbol{r}, t) = \left(\frac{\sigma_3 + \mathrm{i}\sigma_2}{2m}(-\mathrm{i}\hbar\nabla - q\boldsymbol{A}(\boldsymbol{r}, t))^2 + q\phi(\boldsymbol{r}, t) + \sigma_3 mc^2\right)\Psi(\boldsymbol{r}, t). \tag{1}$$

The wave function's components are related by the Pauli matrices σ_2 and σ_3. A possible representation reads

$$\sigma_0 = \begin{pmatrix} 1 & 0 \\ 0 & 1 \end{pmatrix}, \qquad \sigma_1 = \begin{pmatrix} 0 & 1 \\ 1 & 0 \end{pmatrix}, \qquad \sigma_2 = \begin{pmatrix} 0 & -\mathrm{i} \\ \mathrm{i} & 0 \end{pmatrix}, \qquad \sigma_3 = \begin{pmatrix} 1 & 0 \\ 0 & -1 \end{pmatrix}. \tag{2}$$

The physical electromagnetic fields follow from the potentials via

$$\boldsymbol{E}(\boldsymbol{r}, t) = -\nabla\phi(\boldsymbol{r}, t) - \frac{\partial\boldsymbol{A}(\boldsymbol{r}, t)}{\partial t}, \tag{3}$$

$$\boldsymbol{B}(\boldsymbol{r}, t) = \nabla \times \boldsymbol{A}(\boldsymbol{r}, t). \tag{4}$$

Similarly, the Dirac equation, a relativistic generalization of the Pauli equation, is an equation of motion for a four-componet wave function $\Psi(\boldsymbol{r}, t)$ that governs the evolution of a charged spin-half particle. It reads

$$\mathrm{i}\hbar\frac{\partial\Psi(\boldsymbol{r}, t)}{\partial t} = \hat{H}_{\mathrm{D}}(t)\Psi(\boldsymbol{r}, t) = \left(c\boldsymbol{\alpha} \cdot (-\mathrm{i}\hbar\nabla - q\boldsymbol{A}(\boldsymbol{r}, t)) + q\phi(\boldsymbol{r}, t) + mc^2\beta\right)\Psi(\boldsymbol{r}, t) \tag{5}$$

with the matrices $\boldsymbol{\alpha} = (\alpha_1, \alpha_2, \alpha_3)^{\mathsf{T}}$ and β obeying the algebra

$$\alpha_i^2 = \beta^2 = 1, \quad \alpha_i\alpha_k + \alpha_k\alpha_i = 2\delta_{i,k}, \quad \alpha_i\beta + \beta\alpha_i = 0. \tag{6}$$

This algebra determines the matrices α_i and β only up to unitary transforms. In numerical applications, we adopted the so-called Dirac representation with

$$\alpha_1 = \begin{pmatrix} 0 & \sigma_1 \\ \sigma_1 & 0 \end{pmatrix}, \quad \alpha_2 = \begin{pmatrix} 0 & \sigma_2 \\ \sigma_2 & 0 \end{pmatrix}, \quad \alpha_3 = \begin{pmatrix} 0 & \sigma_3 \\ \sigma_3 & 0 \end{pmatrix}, \quad \beta = \begin{pmatrix} \sigma_0 & 0 \\ 0 & -\sigma_0 \end{pmatrix}. \tag{7}$$

While the numerical solution of the time-dependent Schrödinger equation is a mature field with many applications in physics and chemistry relativistic computational quantum dynamics has not yet reached the same degree of maturity. This is partly due to the fact that the interest in solving the relativistic quantum dynamics [18–26] has grown as recently as high-intensity laser facilities where proposed for the near future or even became available providing access to experiments for quantum dynamics in the relativistic regime. Furthermore, attempts to solve the Klein-Gordon or Dirac equation were also hampered by the high computational resources that are required. Numerical procedures propagate quantum wave functions in discrete time steps. The smaller the time step the larger the computational cost. The maximal time step Δt that a numerical procedure may take is limited by the typical energy $\tilde{E}$ of the system under consideration [13], viz. $\Delta t \leq \pi\hbar/|\tilde{E}|$. In relativistic quantum dynamics, we have typical energies of the order $\pm mc^2$ whereas for the nonrelativistic dynamics the restmass energy is irrelevant. Assuming the ground state energy of a hydrogen atom and the restmass energy of an electron as typical energy scales of nonrelativistic and relativistic quantum dynamics we find $\Delta t \leq 48$ as and $\Delta t \leq 0.0013$ as, respectively. Thus, solving the time-dependent Klein-Gordon or Dirac equation for a given time interval requires a number of time steps that is several orders of magnitude larger than for the nonrelativistic Schrödinger equation.

A partial solution to this problem is provided by the Foldy-Wouthuysen transformation [27] which transforms the Dirac equation (5) into block diagonal form. In leading order the new Hamiltonian reads with $\boldsymbol{\sigma} = (\sigma_1, \sigma_2, \sigma_3)^{\mathsf{T}}$

$$\begin{aligned} \hat{H}_{\mathrm{D}}'(t) = {}& \beta\left(mc^2 + \frac{1}{2m}(-\mathrm{i}\hbar\nabla - q\boldsymbol{A}(\boldsymbol{r}, t))^2 - \frac{q\hbar}{2m}\boldsymbol{\sigma} \cdot \boldsymbol{B}(\boldsymbol{r}, t)\right) + q\phi(\boldsymbol{r}, t) \\ & - \beta\left(\frac{1}{8m^3c^2}(-\mathrm{i}\hbar\nabla - q\boldsymbol{A}(\boldsymbol{r}, t))^4 + \frac{q^2\hbar^2}{8m^3c^2}\boldsymbol{B}(\boldsymbol{r}, t)^2 - \frac{q\hbar}{8m^3c^2}\left\{\boldsymbol{\sigma} \cdot \boldsymbol{B}(\boldsymbol{r}, t), (-\mathrm{i}\hbar\nabla - q\boldsymbol{A}(\boldsymbol{r}, t))^2\right\}\right) \\ & - \frac{q\hbar^2}{8m^2c^2}\nabla \cdot \boldsymbol{E}(\boldsymbol{r}, t) - \frac{\mathrm{i}q\hbar^2}{8m^2c^2}\boldsymbol{\sigma} \cdot (\nabla \times \boldsymbol{E}(\boldsymbol{r}, t)) - \frac{q\hbar}{4m^2c^2}\boldsymbol{\sigma} \cdot (\boldsymbol{E}(\boldsymbol{r}, t) \times (-\mathrm{i}\hbar\nabla)) + \dots \end{aligned} \tag{8}$$

In this representation, the Dirac equation decouples into two equations for two two-component wave functions having typical energies of order $+mc^2$ and $-mc^2$, respectively. The additive restmass terms $\pm mc^2$ in (8) may be removed by a gauge transform allowing for an efficient numerical solution [28]. However, the representation (8) is of limited practical value. Compared to the
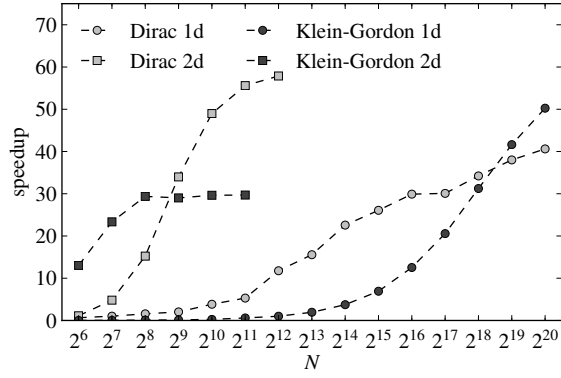
Figure 1: Speedup for propagating a Dirac wave function and a Klein-Gordon wave function over 128 time steps as a function of the grid size. Circles depict results for the one-dimensional Klein-Gordon and Dirac equation on a grid of N data points while squares shows results for the two-dimensional case on a grid of $N \times N$ data points. Performance measurements carried out on a GeForce GTX 480 GPU utilizing the CUFFT library and double precision floating point numbers. A single CPU core (Intel Core i7 CPU at 2.93 GHz) and the FFTW3 library serves as a reference.

original Dirac equation (5) the Hamiltonian (8) is rather complicated although it represents only the first terms of an infinite series. It is applicable in the weakly relativistic limit only. Exact Foldy-Wouthuysen transformations are known for a certain classes of potentials only [29]. Therefore, exact numerical solutions of the time-dependent Klein-Gordon or Dirac equation require high performance computer implementations of numerical propagation schemes or taking advantage of special features of the physical system under consideration.

Aiming for high performance, computer implementations of numerical propagation schemes utilize parallel computing architectures. Currently, there are two major directions of development, multicore architectures with a few (typically two to a few dozen in the near future) general purpose computing units and dedicated accelerators, e. g., graphics processing units (GPUs), with several hundred or more computing units with reduced capabilities each as compared to traditional central processing units (CPUs) [30, 31]. Employing GPUs to perform computations that are traditionally handled by CPUs is commonly referred to as GPU computing [32].

Using Dyson's time ordering operator $\hat{T}$ the formal solution [33] to the time-dependent Klein-Gordon equation and the time-dependent Dirac equation reads

$$\Psi(\boldsymbol{r}, t + \Delta t) = \hat{T} \exp\left(-\frac{\mathrm{i}}{\hbar} \int_t^{t+\Delta t} \hat{H}(t') \, \mathrm{d}t'\right) \Psi(\boldsymbol{r}, t) \,. \tag{9}$$

Usually it is not possible to cast (9) directly into a numerical scheme. Some approximations have to be introduced. Splitting the Hamiltonian $\hat{H}(t)$ into $\hat{H}(t) = \hat{H}_1(t) + \hat{H}_2(t)$ the expression (9) may be expanded into [34]

$$\Psi(\boldsymbol{r}, t + \Delta t) = \underbrace{\exp\left(-\frac{\mathrm{i}}{2\hbar} \int_t^{t+\Delta t} \hat{H}_1(t') \, \mathrm{d}t'\right)}_{= \hat{U}_{\hat{H}_1}(t + \Delta t, t)} \underbrace{\exp\left(-\frac{\mathrm{i}}{\hbar} \int_t^{t+\Delta t} \hat{H}_2(t') \, \mathrm{d}t'\right)}_{= \hat{U}_{\hat{H}_2}(t + \Delta t, t)} \underbrace{\exp\left(-\frac{\mathrm{i}}{2\hbar} \int_t^{t+\Delta t} \hat{H}_1(t') \, \mathrm{d}t'\right)}_{= \hat{U}_{\hat{H}_1}(t + \Delta t, t)} \Psi(\boldsymbol{r}, t) + O\left(\Delta t^3\right) \tag{10}$$

leading to the (Fourier) split operator method [9, 11, 23, 34]. In the case of the Dirac equation we split the Dirac Hamiltonian (5) into

$$\hat{H}_{\mathrm{D},1}(t) = -cq\boldsymbol{\alpha} \cdot \boldsymbol{A}(\boldsymbol{r}, t) + q\phi(\boldsymbol{r}, t) \,, \tag{11a}$$

$$\hat{H}_{\mathrm{D},2}(t) = -\mathrm{i}c\hbar\boldsymbol{\alpha} \cdot \nabla + mc^2\beta \,. \tag{11b}$$

The operator $\hat{U}_{\hat{H}_{\mathrm{D},1}}(t + \Delta t, t)$ is diagonal in real space and $\hat{U}_{\hat{H}_{\mathrm{D},2}}(t + \Delta t, t)$ is diagonal in Fourier space. Thus, the Fourier split operator method propagates $\Psi(\boldsymbol{r}, t)$ alternating in real and in Fourier space, viz.

$$\Psi(\boldsymbol{r}, t + \Delta t) = \hat{U}_{\hat{H}_{\mathrm{D},1}}(t + \Delta t, t) \mathcal{F}^{-1}\left\{\hat{\tilde{U}}_{\hat{H}_{\mathrm{D},2}}(t + \Delta t, t) \mathcal{F}\left\{\hat{U}_{\hat{H}_{\mathrm{D},1}}(t + \Delta t, t) \Psi(\boldsymbol{r}, t)\right\}\right\} + O\left(\Delta t^3\right) \,,$$

where $\hat{\tilde{U}}_{\hat{H}_{\mathrm{D},2}}(t + \Delta t, t)$ denotes the Fourier space representation of $\hat{U}_{\hat{H}_{\mathrm{D},2}}(t + \Delta t, t)$ and $\mathcal{F}\{\cdot\}$ and $\mathcal{F}^{-1}\{\cdot\}$ represent the Fourier transform and its inverse, respectively. From a computational point of view calculating the Fourier transform and its inverse

are the main tasks of the Fourier split operator method. GPUs provide an economically priced hardware platform that allows very efficient implementations of the fast Fourier transform leading to speedup factors of about 40 compared to singe CPU implementations for solving the time-dependent Dirac equation, see figure 1. In the split operator approach to the Klein-Gordon equation we partition (1) into

$$\hat{H}_{\text{KG},1}(t) = q\phi(\boldsymbol{r}, t) + \sigma_3 mc^2 \,, \tag{12a}$$

$$\hat{H}_{\text{KG},2}(t) = \frac{\sigma_3 + i\sigma_2}{2m} \left(-i\hbar\nabla - q\boldsymbol{A}(\boldsymbol{r}, t)\right)^2 \,. \tag{12b}$$

In contrast to the Dirac equation, both operators $\hat{U}_{\hat{H}_{\text{KG},1}}(t + \Delta t, t)$ and $\hat{U}_{\hat{H}_{\text{KG},2}}(t + \Delta t, t)$ can be computed efficiently in real space. Employing a finite difference representation of the operators $\hat{H}_{\text{KG},1}(t)$ and $\hat{H}_{\text{KG},2}(t)$ allows parallel numerical algorithms suitable for distributed memory computers as well as for GPUs. See figure 1 for benchmarks on the real space split operator method for the Klein-Gordon equation. Note that the real space split operator method for the Klein-Gordon equation reaches on a low-cost consumer graphics card a similar performance as on a cluster computer with a few dozen CPU cores [9].

A complementary approach of solving relativistic quantum wave equations is taking advantage of special features of the physical problem under consideration. As an example let us consider a system in the presence of a sinusoidal vector potential

$$\boldsymbol{A}(\boldsymbol{r}, t) = \cos(\boldsymbol{r} \cdot \boldsymbol{k})\boldsymbol{A}(t) \,. \tag{13}$$

In momentum space, this potential couples modes only which are $\hbar\boldsymbol{k}$ apart. Thus, it is legitimate to expand the wave function into a superposition of momentum eigenstates [35] $u_{\boldsymbol{p}}^{\uparrow\downarrow,\pm}e^{i\boldsymbol{p}\cdot\boldsymbol{r}/\hbar}$ of momentum $\boldsymbol{p}$ which are simultaneous energy eigenstates of the free Dirac Hamiltonian with positive (+) or negative (−) energy and spin eigenstates with positive (↑) or negative (↓) spin, viz.

$$\Psi(\boldsymbol{r}, t) = \sum_n \left(c_n^{\uparrow,+}(t)u_{\boldsymbol{p}+n\hbar\boldsymbol{k}}^{\uparrow,+} + c_n^{\downarrow,+}(t)u_{\boldsymbol{p}+n\hbar\boldsymbol{k}}^{\downarrow,+} + c_n^{\uparrow,-}(t)u_{\boldsymbol{p}+n\hbar\boldsymbol{k}}^{\uparrow,-} + c_n^{\downarrow,-}(t)u_{\boldsymbol{p}+n\hbar\boldsymbol{k}}^{\downarrow,-} \right) e^{i(\boldsymbol{p}+n\hbar\boldsymbol{k})\cdot\boldsymbol{r}/\hbar} \,. \tag{14}$$

Plugging the series (14) into the Dirac equation (5) yields an infinite system of ordinary linear differential equations for the expansion coefficients $c_n^{\uparrow\downarrow,\pm}(t)$. The system's coupling matrix has a banded structure. Thus, the time evolution of the expansion coefficients can be calculated efficiently by employing a Crank-Nicolson scheme or Krylov subspace methods. This approach is applicable in particular to stetups with physical states that can be described by a superposition of a small number of momentum eigenstates as in the Kapitza-Dirac effect that we will study in section 4.

3. Tunnel ionization at relativistic laser intensities

The ionization of hydrogen-like ions occurs in the so-called tunneling regime when the laser's electric field amplitude E_0 is smaller than those required for over-the-barrier ionization [36] and the Keldysh parameter $\gamma = \omega\sqrt{2mI_p}/(eE_0)$ is well below unity with the ionization potential I_p, the laser's angular frequency ω and the elementary charge e. In the tunnel-ionization regime the electron travels during its journey from the bound state into the continuum through a region which is forbidden according to classical mechanics. For nonrelativistic dynamics, when the typical electron velocities are small compared to the speed of light, the effect of the laser's magnetic field can be neglected. In this case the well-known intuitive picture for the tunneling dynamics arises in which the electron tunnels out through an effective potential $V_{\text{eff}}(\boldsymbol{r}) = V(\boldsymbol{r}) + \boldsymbol{r} \cdot \boldsymbol{E}(t)$ formed by the atomic potential $V(\boldsymbol{r})$ and the laser's oscillating electric field $\boldsymbol{E}(t)$.

However, the contribution of the laser's magnetic field component can no longer be neglected when we enter the relativistic regime. A transverse laser field with perpendicular electric and magnetic components can not be described solely by a scalar potential, a vector potential is required which does not appear in the conventional tunneling picture. Consequently, a generalization of the tunneling picture into the relativistic regime is not straightforward and there is no clear intuitive picture for the relativistic quasi-static ionization dynamics in the classically forbidden region. In the following we will establish a tunneling picture that incorporates the vector potential by quasi-classical considerations. Predictions by this quasi-classical picture will be verified by a numerical solution of the time-dependend Dirac equation.

We describe the laser field via its vector potential in electric field gauge [37, 38], i.e., $\phi(\boldsymbol{r}, t) = -\boldsymbol{r} \cdot \boldsymbol{E}(\eta)$ and $\boldsymbol{A}(\boldsymbol{r}, t) = -\hat{\boldsymbol{k}}[\boldsymbol{r} \cdot \boldsymbol{E}(\eta)]/c$ with the laser phase $\eta = t - z/c$, the electron's coordinate $\boldsymbol{r} = (x, y, z)$, the unit vector in laser propagation direction $\hat{\boldsymbol{k}}$, and the speed of light c. In order to study the effect of the vector potential we consider the static Hamiltonian at maximal laser field strength

$$H = \frac{p_x^2}{2m} + \frac{p_y^2}{2m} + \frac{(p_z - qxE_0/c)^2}{2m} + V(r) + qxE_0 \,, \tag{15}$$

with the electron's charge $q = -e$, the canonical momenta p_x, p_y, and p_z and $r = \sqrt{x^2 + y^2 + z^2}$. By virtue of the electric field gauge the Hamilton function equals the total energy $-I_p$. The tunneling dynamics takes place in close vicinity along the x-axis (the polarization direction). Therefore, the atomic-potential's central force in the direction of the y-axis and the z-axis (the laser's propagation directions) is negligible in the tunneling region and the canonical momenta p_y and p_z become approximately conserved. Consequently, the electron dynamics is separable and the equation $H = -I_p$ can be written as

$$-I_p - \left(\frac{p_y^2}{2m} + \frac{(p_z - qxE_0/c)^2}{2m} \right) = \frac{p_x^2}{2m} + (V(x) + qxE_0) . \tag{16}$$

Equation (16) is the desired generalization of the nonrelativistic one-dimensional model of tunnel ionization [36]. According to this generalized model, the electron propagates along the laser polarization direction through the barrier $V_{\text{eff}}(x) = V(x) + qxE_0$ with a position dependent total energy

$$\mathcal{E}(x) = -I_p - \left(\frac{p_y^2}{2m} + \frac{(p_z - qxE_0/c)^2}{2m} \right), \tag{17}$$

which is the difference between the binding energy and the kinetic energy of the motion in the propagation direction of the laser.

With (16) we find the momentum in electric field direction $p_x(x) = \mathrm{i} \sqrt{2m[V_{\text{eff}}(x) - \mathcal{E}(x)]}$. The WKB tunneling probability is proportional to $\exp(-\Gamma)$, where Γ is given by the integral

$$\Gamma = -\frac{2\mathrm{i}}{\hbar} \int_{x_i}^{x_e} p_x(x) \, \mathrm{d}x \tag{18}$$

over the classical forbidden region $x_i \leq x \leq x_e$, i.e., where $V_{\text{eff}}(x) > \mathcal{E}(x)$. Note that the effective potential depends on the canonical momenta in y- and z-direction. The WKB tunneling probability is maximal for $p_y = 0$ and $p_z = p_z^*$. Thus, the most probable kinematic momenta with witch the electron enters and leaves the barrier are $p_{z,\text{kin}}(x_i) = p_z^* - qx_iE_0/c$ and $p_{z,\text{kin}}(x_e) = p_z^* - qx_eE_0/c$, respectively. Figure 2 (left panel) displays the WKB tunneling probability as a function of the canonical momentum p_z. The WKB tunneling probability is maximal for $p_z^* \approx -2I_P/(3c)$ yielding a kinematic momentum $p_{z,\text{kin}} \approx I_p/(3c)$ at the tunneling exit. Thus, the quasi-classical model predicts that electrons leave the tunneling barrier with non-zero momentum in propagation direction of the laser as a consequence of the laser's magnetic field component. This may be interpreted as a momentum transfer due to the Lorentz force acting on the Keldysh-time scale τ_K during tunneling. Numerical simulations support the prediction of a momentum transfer. Figure 2 (right panel) shows the distribution of the canonical momentum at maximal laser intensity. The momentum distribution consits of the bound part which is symmetric around zero momentum and the ionized part at about $p_z = p_z^*$. Note that in contrast to the quasi-classical model our numerical simulation includes all relativistic effects not only magnetic dipole effects. In fact, one can show that relativistic effects that go beyond magnetic dipole effects change the overall tunneling probability but do not affect the relativistic tunneling picture as outlined above [15]. Examining the wave function in position space we find by a numerical solution of the Dirac equation and quantum mechanical analytical calculations that the wave function is also shifted during tunneling under the barrier into propagation direction of the laser by about $\tau_E p_{z,\text{kin}}(x_e)$ with the Eisenbud-Wigner-Smith time delay τ_E [15], i.e., the time the electron spends under the barrier.
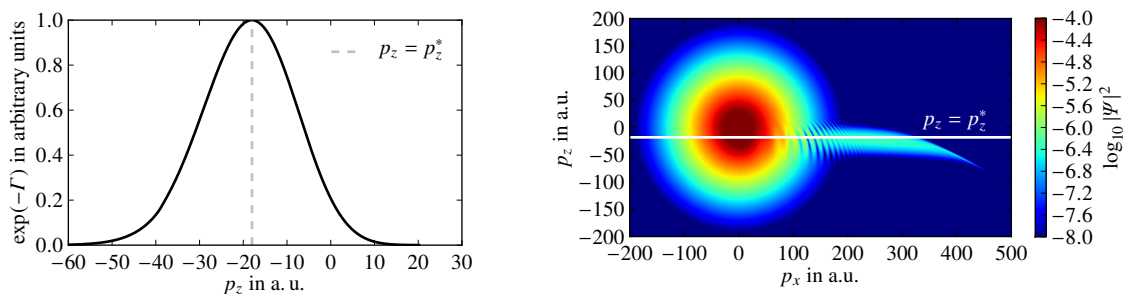

Figure 2: Left panel: WKB tunneling probability for an electron in a two-dimensional soft-core potential (serving as a model for highly charged hydrogen-like ions) exposed to a strong laser field as a function of the canonical momentum in laser propagation direction p_z. The tunneling probability is maximal at $p_z = p_z^*$. Right panel: The momentum space distribution of the corresponding wave function. The density's portion at $p_z \approx p_z^*$ represents the tunneled part of the electronic wave function. The applied parameters are $I_p/(mc^2) = 1/4$ and $E_0/E_a = 1/30$ with $E_a = 5.14 \cdot 10^{11}$ V/m denoting the characteristic atomic field strength.
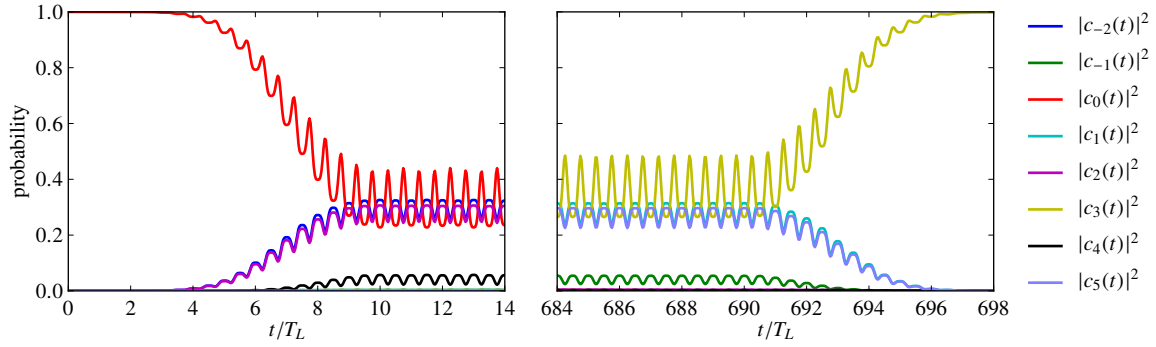
Figure 3: Occupation of different momentum states $|c_n(t)|^2 = |c_n^{\uparrow+}(t)|^2 + |c_n^{\downarrow+}(t)|^2 + |c_n^{\uparrow-}(t)|^2 + |c_n^{\downarrow-}(t)|^2$ as a function of time t measured in units of the lasers period T_L. Laser parameters of this simulation correspond to two counterpropagating X-ray laser beams with a peak intensity of $2.0 \times 10^{23}\,\text{W/cm}^2$ each and a photon energy of 3.1 keV. The electron impinges at an angle of inclination of $\vartheta = 0.4°$ and a momentum of $176\,\text{keV}/c$, in order to fulfill the Bragg condition (22).

4. Kapitza-Dirac scattering at relativistic laser intensities

The diffraction of an electron beam from a standing wave of light is referred to as the Kapitza-Dirac effect [39, 40]. It highlights the electron's quantum wave nature and may be interpreted as an analogue of the optical diffraction of light on a massive grating, but with the roles of light and matter interchanged. In order to study Kapitza-Dirac scattering at relativistic laser intensities we consider a quantum electron wave packet in a standing linearly polarized light wave with maximal electric field strength $\boldsymbol{E}$, wave vector $\boldsymbol{k}$, and wavelength $\lambda = 2\pi/|\boldsymbol{k}| = 2\pi/k$, respectively. The laser is modeled by the vector potential

$$\boldsymbol{A}(\boldsymbol{r}, t) = -\frac{\boldsymbol{E}}{ck}\cos(\boldsymbol{k} \cdot \boldsymbol{r})\sin(ckt)w(t) \tag{19}$$

introducing the speed of light c and the temporal envelope function $w(t)$. The relativistic quantum dynamics of an electron with mass m and charge $-e$ is governed by the Dirac equation (5). Employing the ansatz (14) and the potential (19) the Dirac equation yields a system of ordinary differential equations

$$i\hbar\dot{c}_n^\gamma(t) = \varepsilon^\gamma \mathcal{E}(\boldsymbol{p} + n\hbar\boldsymbol{k})c_n^\gamma(t)$$
$$- \frac{w(t)e\sin(ckt)}{2k}\sum_\zeta \left(\langle u_{\boldsymbol{p}+n\hbar\boldsymbol{k}}^\gamma | \boldsymbol{E} \cdot \boldsymbol{\alpha} | u_{\boldsymbol{p}+(n-1)\hbar\boldsymbol{k}}^\zeta \rangle c_{n-1}^\zeta(t) + \langle u_{\boldsymbol{p}+n\hbar\boldsymbol{k}}^\gamma | \boldsymbol{E} \cdot \boldsymbol{\alpha} | u_{\boldsymbol{p}+(n+1)\hbar\boldsymbol{k}}^\zeta \rangle c_{n+1}^\zeta(t) \right), \tag{20}$$

where we have introduced the relativistic energy momentum dispersion relation $\mathcal{E}(\boldsymbol{p}) = \sqrt{m^2c^4 + c^2\boldsymbol{p}^2}$ and the signum ε^γ, which is 1 for $\gamma \in \{\uparrow +, \downarrow +\}$ and -1 for $\gamma \in \{\uparrow -, \downarrow -\}$. The electron that is incident to the laser is modeled by a positive-energy plane wave with momentum $\boldsymbol{p}$ and definite spin. This means the initial condition for (20) is

$$c_n^\gamma(0) = \begin{cases} 1 & \text{if } n = 0 \text{ and } \gamma = \uparrow +, \\ 0 & \text{else.} \end{cases} \tag{21}$$

Electron diffraction by light may be observed only if the electron's momentum and the photon momenta of the laser meet a Bragg condition. Considering classical energy and momentum conservation [16] yields

$$\frac{\cos\vartheta}{\lambda_p} = -\frac{n_r - n_l}{2\lambda} + \frac{n_r - n_l}{|n_r - n_l|}\frac{n_r + n_l}{2}\sqrt{\frac{1}{\lambda^2} - \frac{1}{n_r n_l}\left(\frac{\sin^2\vartheta}{\lambda_p^2} + \frac{1}{\lambda_C^2}\right)} \tag{22}$$

with ϑ denoting the angle between $\boldsymbol{p}$ and $\boldsymbol{k}$, the de Broglie wavelength $\lambda_p = 2\pi\hbar/|\boldsymbol{p}|$, and the Compton wavelength $\lambda_C = 2\pi\hbar/(mc)$. The integers n_r and n_l are the net numbers of photons exchanged with the right- and left-traveling laser waves, respectively, with positive (negative) values indicating photon absorption (emission). To be consistent with the nonrelativistic limit n_r and n_l must have opposite signs. As a consequence of (22) the initial electron momentum $\boldsymbol{p}$ and/or the laser's photon momentum $\hbar k$ must be of the order of mc, i. e., relativistic, unless the electron scatters elastically, i. e., $n_r + n_l = 0$, or the electron interacts with a very large number of photons, i. e., $|n_r| + |n_l| \gg 0$.
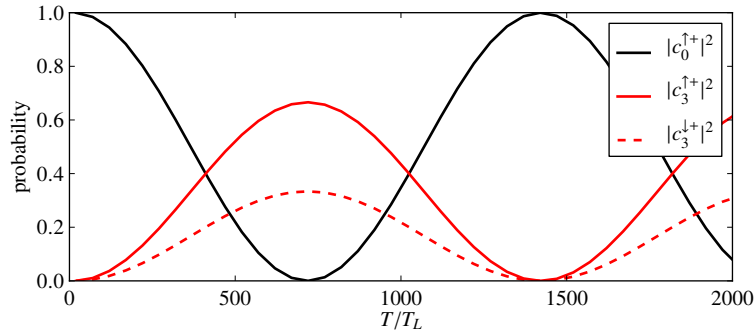
Figure 4: Spin resolved occupation probabilities as a function of the interaction time T for a three-photon Kapitza-Dirac effect (adopted from Phys. Rev. Let., vol. 109, article 043601, 2012). Experimental parameters as in figure 3. The occupation probabilities oscillate in Rabi cycles with a period that is about 1500 times larger than the laser period.

Figure 3 shows a typical time evolution of the occupation of different momentum states for a setup that meets the Bragg condition for three-photon scattering with $n_r = 2$ and $n_l = -1$. Initially the mode with momentum $\boldsymbol{p}$ is occupied only. During the interaction with the laser other modes get occupied as well and after a smooth turn-off phase the mode with momentum $\boldsymbol{p} + 3\hbar\boldsymbol{k}$ is occupied with probability one. Generally the end state depends on the total interaction time T. Numerical simulations show that the occupation probabilities oscillate in Rabi cycles [16]. In the laser field the probabilities $|c_n^\gamma(t)|^2$ oscillate on two time scales, a short scale which is given by the laser period T_L and a large scale which is given by the Rabi period T_R. The effect of the fast oscillations disappears when the electron leaves the laser field while the effect of the slow variation can be measured in the electron's momentum distribution outside the laser leading to the Kapitza-Dirac effect, see figure 3 right panel. Figure 4 shows the occupation probability $|c_n^\gamma(t)|^2$ as a function of the total interaction time T that means when electron is field-free. Because experimental parameters have been chosen such that the three-photon Bragg condition is met the occupation probability oscillates between $|c_0^{\uparrow+}(t)|^2$ and $|c_3^{\uparrow\downarrow+}(t)|^2$. Note that when the electron has absorbed three photons from the laser field the electron is in a superposition of spin-up and spin-down states although the electron beam enters the laser spin-polarized along the direction of the laser's electric field component [16]. Thus, three-photon Kapitza-Dirac scattering induces oscillation of the spin.

[1] V. Yanovsky, V. Chvykov, G. Kalinchenko, P. Rousseau, T. Planchon, T. Matsuoka, A. Maksimchuk, J. Nees, G. Cheriaux, G. Mourou, and K. Krushelnick, "Ultra-high intensity- 300-TW laser at 0.1 Hz repetition rate," *Optics Express* **16**(3), pp. 2109–2114, 2008.

[2] A. Di Piazza, C. Müller, K. Z. Hatsagortsyan, and C. H. Keitel, "Extremely high-intensity laser interactions with fundamental quantum systems," *Reviews of Modern Physics* **84**, pp. 1177–1228, 2012.

[3] V. G. Bagrov and D. Gitman, *Exact Solutions of Relativistic Wave Equations*, vol. 39 of *Mathematics and Its Applications*, Springer, 1990.

[4] F. Gross, *Relativistic Quantum Mechanics and Field Theory*, Wiley & Sons, 1999.

[5] P. Strange, *Relativistic Quantum Mechanics With Applications in Condensed Matter and Atomic Physics*, Cambridge University Press, 1998.

[6] F. Schwabl, *Advanced Quantum Mechanics*, Springer, 4th ed., 2008.

[7] A. Wachter, *Relativistic Quantum Mechanics*, Springer, 1st ed., 2009.

[8] F. Ehlotzky, K. Krajewska, and J. Z. Kamiński, "Fundamental processes of quantum electrodynamics in laser fields of relativistic power," *Reports on Progress in Physics* **72**(4), pp. 1–32, 2009.

[9] M. Ruf, H. Bauke, and C. H. Keitel, "A real space split operator method for the Klein-Gordon equation," *Journal of Computational Physics* **228**(24), pp. 9092–9106, 2009.

[10] F. Blumenthal and H. Bauke, "A stability analysis of a real space split operator method for the Klein-Gordon equation," *Journal of Computational Physics* **231**(2), pp. 454–464, 2012.

[11] H. Bauke and C. H. Keitel, "Accelerating the Fourier split operator method via graphics processing units," *Computer Physics Communications* **182**(12), pp. 2454–2463, 2011.

[12] H. Bauke and S. Mertens, *Cluster Computing*, Springer, Heidelberg, 2005.

[13] H. Bauke and C. H. Keitel, "Canonical transforms and the efficient integration of quantum mechanical wave equations," *Physical Review E* **80**(1), p. 016706, 2009.

[14] R. E. Wagner, M. R. Ware, B. T. Shields, Q. Su, and R. Grobe, "Space-time resolved approach for interacting quantum field theories," *Physical Review Letters* **106**(2), p. 023601, 2001.

[15] M. Klaiber, E. Yakaboylu, H. Bauke, K. Z. Hatsagortsyan, and C. H. Keitel, "Under-the-barrier dynamics in laser-induced relativistic tunneling." arXiv:1205.2004, accepted for publication in Physical Review Letters.

[16] S. Ahrens, H. Bauke, C. H. Keitel, and C. Müller, "Spin dynamics in the Kapitza-Dirac effect," *Physical Review Letters* **109**(4), p. 043601,

2012.

[17] H. Feshbach and F. Villars, "Elementary relativistic wave mechanics of spin 0 and spin 1/2 particles," *Reviews of Modern Physics* **30**(1), pp. 24–45, 1958.

[18] N. J. Kylstra, A. M. Ermolaev, and C. J. Joachain, "Relativistic effects in the time evolution of a one-dimensional model atom in an intense laser field," *Journal of Physics B: Atomic, Molecular and Optical Physics* **30**, pp. L449–L460, 1997.

[19] U. W. Rathe, C. H. Keitel, M. Protopapas, and P. L. Knight, "Intense laser-atom dynamics with the two-dimensional Dirac equation," *Journal of Physics B* **30**(15), pp. L531–L539, 1997.

[20] R. Taïeb, V. Véniard, and A. Maquet, "Signature of relativistic effects in atom-laser interactions at ultrahigh intensities," *Physical Review Letters* **81**(14), pp. 2882–2885, 1998.

[21] J. W. Braun, Q. Su, and R. Grobe, "Numerical approach to solve the time-dependent dirac equation," *Physical Review A* **59**(1), pp. 604–612, 1999.

[22] G. R. Mocken and C. H. Keitel, "Quantum dynamics of relativistic electrons," *Journal of Computational Physics* **199**(2), pp. 558–588, 2004.

[23] G. R. Mocken and C. H. Keitel, "FFT-split-operator code for solving the Dirac equation in 2 + 1 dimensions," *Computer Physics Communications* **178**(11), pp. 868–882, 2008.

[24] S. Selstø, E. Lindroth, and J. Bengtsson, "Solution of the Dirac equation for hydrogenlike systems exposed to intense electromagnetic pulses," *Physical Review A* **79**(4), p. 043418, 2009.

[25] F. Fillion-Gourdeau, E. Lorin, and A. D. Bandrauk, "Numerical solution of the time-dependent Dirac equation in coordinate space without fermion-doubling," *Computer Physics Communications* **183**(7), pp. 1403–1415, 2012.

[26] Y. V. Vanne and A. Saenz, "Solution of the time-dependent dirac equation for multiphoton ionization of highly charged hydrogenlike ions," *Physical Review A* **85**(3), p. 033411, 2012.

[27] L. L. Foldy and S. A. Wouthuysen, "On the Dirac theory of spin 1/2 particles and its non-relativistic limit," *Physical Review* **78**(1), pp. 29–36, 1950.

[28] S. X. Hu and C. H. Keitel, "Dynamics of multiply charged ions in intense laser fields," *Physical Review A* **63**(5), p. 053402, 2001.

[29] A. G. Nikitin, "On exact Foldy-Wouthuysen transformation," *Journal of Physics A: Mathematical and General* **31**(14), pp. 3297–3300, 1998.

[30] D. Kirk and W. Hwu, *Programming Massively Parallel Processors: A Hands-on Approach*, Morgan Kaufmann, 2010.

[31] V. Kindratenko, R. Wilhelmson, R. Brunner, T. J. Martïnez, and W. Hwu, "High-performance computing with accelerators," *Computing in Science & Engineering* **12**(4), pp. 12–16, 2010.

[32] J. Owens, M. Houston, D. Luebke, S. Green, J. Stone, and J. Phillips, "GPU computing," *Proceedings of the IEEE* **96**(5), pp. 879–899, 2008.

[33] P. Pechukas and J. C. Light, "On the exponential form of time-displacement operators in quantum mechanics," *The Journal of Chemical Physics* **44**(10), pp. 3897–3912, 1966.

[34] M. D. Feit, J. A. Fleck, Jr., and A. Steiger, "Solution of the Schrödinger equation by a spectral method," *Journal of Computational Physics* **47**(3), pp. 412–433, 1982.

[35] B. Thaller, *Advanced Visual Quantum Mechanics*, Springer, 2004.

[36] S. Augst, D. Strickland, D. D. Meyerhofer, S. L. Chin, and J. H. Eberly, "Tunneling ionization of noble gases in a high-intensity laser field," *Physical Review Letters* **63**(20), pp. 2212–2215, 1989.

[37] H. R. Reiss, "Field intensity and relativistic considerations in the choice of gauge in electrodynamics," *Physical Review A* **19**(3), pp. 1140–1150, 1979.

[38] G. Grynberg, A. Aspect, and C. Fabre, *Introduction to Quantum Optics: From the Semi-classical Approach to Quantized Light*, Cambridge University Press, Cambridge, 2010.

[39] P. L. Kapitza and P. A. M. Dirac, "The reflection of electrons from standing light waves," *Math. Proc. Cambridge Philos. Soc.* **29**(2), pp. 297–300, 1933.

[40] H. Batelaan, "Illuminating the Kapitza-Dirac effect with electron matter optics," *Reviews of Modern Physics* **79**(3), pp. 929–941, 2007.